



Silica Nanoparticles Induce Hepatotoxicity by Triggering Oxidative Damage, Apoptosis, and Bax-Bcl2 Signaling Pathway

Bakhta Aouey¹ · Khadija Boukholda¹ · Brahim Gargouri¹ · Harsharan S. Bhatia^{2,3} · Abdelraheim Attaai⁴ · Mohamed Kebieche^{5,6} · Michèle Bouchard⁷ · Hamadi Fetoui¹

Received: 10 April 2021 / Accepted: 28 May 2021

© The Author(s), under exclusive licence to Springer Science+Business Media, LLC, part of Springer Nature 2021

Abstract

The increase in the usage of silica nanoparticles (SiNPs) in the industrial and medical fields has raised concerns about their possible adverse effects on human health. The present study aimed to investigate the potential adverse effects of SiNPs at daily doses of 25 and 100 mg/kg body weight intraperitoneally (i.p.) for 28 consecutive days on markers of liver damage in adult male rats. Results revealed that SiNPs induced a marked increase in serum markers of liver damage, including lactate dehydrogenase (LDH), alanine aminotransferase (ALAT), and aspartate aminotransferase (ASAT). SiNPs also induced an elevation of reactive oxygen species (ROS) production in liver, along with an increase in oxidative stress markers (NO, MDA, PCO, and H₂O₂), and a decrease in antioxidant enzyme activities (CAT, SOD, and GPx). Quantitative real-time PCR showed that SiNPs also induced upregulation of pro-apoptotic gene expression (including *Bax*, *p53*, *Caspase-9/3*) and downregulation of anti-apoptotic factors *Bcl-2*. Moreover, histopathological analysis revealed that SiNPs induced hepatocyte alterations, which was accompanied by sinusoidal dilatation, Kupffer cell hyperplasia, and the presence of inflammatory cells in the liver. Taken together, these data showed that SiNPs trigger hepatic damage through ROS-activated caspase signaling pathway, which plays a fundamental role in SiNP-induced apoptosis in the liver.

Keywords Silica nanoparticles · ROS · Caspase · Hepatotoxicity · Apoptosis

✉ Hamadi Fetoui
fetoui_hamadi@yahoo.fr

¹ Laboratory of Toxicology-Microbiology and Environmental Health (17ES06), Faculty of Sciences of Sfax, University of Sfax, BP1171, 3000 Sfax, Tunisia

² Institute for Tissue Engineering and Regenerative Medicine (iTERM), Helmholtz Zentrum München, 85764 Neuherberg, Germany

³ Institute for Stroke and Dementia Research, Klinikum Der Universität München, Ludwig Maximilian University of Munich (LMU), 81377 Munich, Germany

⁴ Department of Anatomy and Histology, Faculty of Veterinary Medicine, Assiut University, Assiut, Egypt

⁵ Laboratory of Cellular and Molecular Biology, University of Mohamed Seddik Ben Yahia, Jijel, Algeria

⁶ Faculty of Natural and Life Sciences, LBMBPC, University of Batna 2, 05078 Fesdis, Batna2, Algeria

⁷ Department of Environmental and Occupational Health, Chair in Toxicological Risk Assessment and Management, and Public Health Research Center (CReSP), University of Montreal, Roger-Gaudry Building, U424Main Station, P.O. Box 6128, Montreal, Quebec H3C 3J7, Canada

Introduction

Silica nanoparticles (SiNPs) have been widely used in biomedicine for drug delivery, imaging, cell tracking, and photothermal therapy due to their unique characteristics, including large surface area, high structural stability, easy surface functionalization, low production costs, excellent biocompatibility, and protracted circulation properties [12, 32]. Given the rapid development of nanotechnology and the use of silica particles in the nanoscale, there have been concerns about their potential toxicity. Previous studies showed that SiNPs administered to rodents distributed in various peripheral organs, including the liver, spleen, lungs, and kidneys [40, 42] and could perturb various physiological systems, such as cardiovascular, nervous, reproductive, and immune systems [45, 61]. In particular, a recent study by Balli et al. [8] showed that silica can cause toxic effects in the brain, liver, and kidneys of rats after exposure to SiNPs of different sizes (6, 20, and 50 nm). Additionally, in vivo experiments have shown that intravenous exposure to SiNPs caused histopathological alterations and functional impairments in the

liver [11]. However, the underlying molecular mechanism leading to such toxicological effects induced by SiNPs exposure is poorly elucidated [60].

During the interaction of cells, SiNP was shown to cause membrane destabilization, which leads to protein oxidation, enzyme inactivation, DNA damage, and finally cell death [53]. In recent years, a large number of *in vitro* investigations also demonstrated that SiNPs can induce oxidative stress in different cell lines [25, 49]. Elevated oxidative stress can collapse the mitochondrial membrane potential ($\Delta\psi_m$), induce cytochrome c release from mitochondria to cytoplasm, activating mitochondria-dependent apoptotic signaling [26, 31]. Several genes are known to control the apoptotic pathway and act as death switches. The p53 gene is known as the guardian of the genome and induces cell cycle arrest or apoptosis in response to DNA damage [20, 54]. The Bcl-2 and Bax are two distinct members of a gene family that play a crucial role in apoptosis [7]. These proteins can both act as anti-apoptotic and pro-apoptotic regulators. An increase in the ratio of Bax/Bcl-2 is indicative of cell death switch, leading to apoptosis [18]. Furthermore, apoptotic stimuli leading to destabilization of the mitochondrial integrity precedes activation of caspases, which play a central role in the execution of apoptosis [44]. To date, reports on hepatotoxicity of SiNPs mainly focus on the morphometric alterations, hematological alterations, inflammation, and fibrosis in the liver [5, 36]. However, the manner in which liver cells respond to SiNPs is yet to be elucidated in *in vivo* studies.

Therefore, the current study aimed to investigate the hepatic histopathology and oxidative stress induced by subacute exposure to SiNPs in rats and to elucidate the relationship between oxidative damage and intrinsic apoptotic pathways.

Materials and Methods

Chemicals

Spherical and porous silica powder (SiNPs) particles were prepared from Sigma Chemicals Aldrich (Deisenhofen, Germany). XRD results showed that SiNPs are in amorphous form with a primary size of 15 nm. Purification of SiNPs was determined as 99.5% with a surface area of 640 m²/g. All chemical products used for biochemical assays were obtained from Sigma Chemicals Aldrich (Deisenhofen, Germany).

Preparation of Silica Nanoparticles

SiNPs were suspended in deionized water at 37 °C. Nanoparticles were dispersed by ultrasonication (Sonorex RK 52 H, Bandelin, Germany) for 15 min before being diluted

immediately before use. Nanoparticle solution was prepared so that the necessary dose could be administered intraperitoneally (i.p.).

Experimental Animals

Adult male Wistar rats aged between 7 and 8 weeks old and weighing about 220 ± 20 g were obtained from the Central Pharmacy of Tunis (SIPHAT, Tunisia). The animals were put in plastic cages located in a well-ventilated vivarium and with a 12-h light: dark cycle; they also had free access to food and water throughout the experiment [21]. After a period of acclimatization, animals were randomly divided into three groups of ten rats each ($n = 10$): group 1 serving as controls received an injection of sterile water by intraperitoneal way; group 2 was treated with a low dose of SiNPs of 25 mg/kg bw; group 3 was treated with a high dose of SiNPs of 100 mg/kg bw. Doses used in this study represent (1/200 DL50 and 1/50 DL50, respectively) of SiNPs [51]. SiNPs were injected once daily for 28 consecutive days. All animal procedures were approved by the local Ethics Committee of the Faculty of Sfax and performed in strict accordance with Ethical principles and guidelines for experiments on animals.

Biochemical Analysis

At the end of the study, control and treated animals were euthanized by cervical decapitation to avoid stress conditions. Blood was collected and serum was separated by centrifugation. The serum was kept at −80 °C until analysis for the assessment of hepatic biomarkers (ALAT, ASAT, and LDH) using reagent kits from Biomaghreb (Ariana, Tunis, Tunisia). Livers were excised, washed with ice-cold physiological saline, and weighed. Portions were taken for histopathological studies and the remaining parts of livers were homogenized in 0.1 M phosphate buffer (pH = 7.4). The supernatants were separated, aliquoted, and stored at −80 °C until analysis.

Determination of Enzymatic and Non-enzymatic Antioxidant Activities in the Liver

Catalase (CAT) activity was assayed by the decomposition of hydrogen peroxide (H₂O₂) according to the method of Aebi [2]. A decrease in absorbance due to H₂O₂ degradation was monitored at 240 nm for 1 min and the enzyme activity was expressed as μmol H₂O₂ consumed/min/mg protein.

Total superoxide dismutase activity (SOD) was evaluated by measuring the inhibition of pyrogallol activity as described by Marklund and Marklund [37]. One unit (U) corresponded to the enzyme activity required to inhibit the

half of pyrogallol oxidation. SOD activity was expressed as U/mg protein.

Glutathione peroxidase activity (GPx) was measured according to Flohe and Gunzler [22]. The enzyme activity was expressed as nmol of GSH oxidized/min/mg protein.

Reduced glutathione in the liver was determined by the method of Ellman [17] based on the development of a yellow color when 5,5-dithiobis-2-nitrobenzoic acid (DTNB) was added to compounds containing sulfhydryl groups. The absorbance was measured at 412 nm after 10 min using a microplate reader. Total GSH content was expressed as nmol/mg protein.

Determination of Oxidative Stress Markers in the Liver

Lipid peroxidation in the hippocampus tissue was estimated colorimetrically by measuring thiobarbituric acid reactive substances (TBARS), which were expressed in terms of malondialdehyde contents according to Draper and Hadley [14] method. Briefly, 100 μ L of trichloroacetic acid (5%) was added to 100 μ L of hippocampus supernatants and centrifuged at $4000 \times g$ for 10 min. One hundred microliters of the supernatants were transferred into Pyrex tubes and incubated with 200 μ L of thiobarbituric acid reagent (TBA, 0.67%) in a water bath at 90 °C for 15 min. The TBARS were determined using a microplate reader at 532 nm. MDA values were calculated using 1,1,3,3-tetraethoxypropane as the standard and expressed as nmoles of MDA/mg protein.

Protein carbonyl (PCO) contents were detected by the reaction with 2,4-dinitrophenylhydrazine (DNPH) as reported by Levine et al. (1990). Briefly, the DNPH reaction proteins were precipitated with an equal volume of 20% (w/v) trichloroacetic acid and washed three times with 2 mL of an ethanol/ethyl acetate mixture (1:1). Finally, the precipitates were dissolved in a 6 M guanidine HCl solution. The absorbance was measured at 370 nm using the molar extinction coefficient of DNPH, $\epsilon = 22,000 \text{ M}^{-1} \text{ cm}^{-1}$ and results were expressed as nmol/mg protein.

Hydroperoxide assay (H_2O_2) was determined by the method of Gay et al. [23]. Briefly, 50 μ L of the sample was added to 950 μ L of FOX 1 reagent (25 mM sulfuric acid, 250 μ M ferrous ammonium sulfate, 100 μ M xylenol orange, and 0.1 M sorbitol) and incubated for 30 min at room temperature. This assay is based on the ability of H_2O_2 to oxidize the ferrous Fe^{2+} ions to the ferric Fe^{3+} ions, which react with xylenol orange to form a colored complex. The absorbance of the samples was read at 570 nm and the concentration of H_2O_2 was determined using standard peroxide solutions in the same microtiter plate.

Nitric oxide production was determined based on the Griess reaction [24]. Briefly, 50 μ L of deproteinized sample was incubated with 50 μ L of the Griess reagent at room temperature for 10 min. Absorbance was measured at 550 nm

using a microplate reader. Nitrite concentration was determined from a standard nitrite curve generated using NaNO_2 . Results were expressed as $\mu\text{mol/mg protein}$.

Measurement of ROS Production in the Liver

Levels of oxygen reactive species in the liver of rats were measured according to the method of [15]. The supernatant was incubated with 10 μ L of 5 mM 2',7'-dichlorofluorescein diacetate (DCHF-DA). Levels of oxygen reactive species levels were determined by a spectrofluorimetric method, using DCHF-DA assay. The oxidation of DCHF-DA to fluorescent dichlorofluorescein was measured for the detection of intracellular oxygen reactive species. The fluorescence intensity was measured using a fluorescence plate reader with an excitation wavelength of 485 nm and emission detection at 530 nm.

Protein Quantification

The protein content of the tissues was measured by the method of Bradford [10],

RNA Isolation and Real-Time RT-PCR

Total RNA was extracted using the iScript™ RT-qPCR sample preparation reagent and according to the manufacturer's instructions (170–8898, Bio-Rad)). RNA concentrations and purity were determined by measuring the A260/280 absorbance ratios using NanoPhotometer™ (Implen, GmbH). The synthesized cDNA was the template for real-time qPCR amplification carried out by the CFX96 real-time PCR detection system using iQ SYBR supermix (Bio-Rad Laboratories GmbH, Munich, Germany) [6]. Lists of primer sequences of Bax, Bcl-2, P53, Caspase-3, and Caspase-9 are listed in Table 1. The $2^{-\Delta\Delta\text{Ct}}$ method was used to analyze the relative changes in gene expression [33]. Data were normalized to the housekeeping gene β -actin.

Semiquantitative Histopathological Evaluation of Hepatic Tissue

Liver tissues from the control and treated rats were fixed in 10% buffered formalin and were processed for paraffin sectioning. Sections of 5 μ m thickness were stained with hematoxylin and eosin (H&E) and examined with a Leica® microscope fitted with a Sony® digital camera to capture images for histological studies. A semiquantitative evaluation was performed in examined fields ($n = 10$) according to the percentage, degree, and extent of tissue damage and was scored according to Michael [39] as follows: (–), normal appearance (absence of pathological lesion 0%), (+), mild

Table 1 Sequence of all primer used in RT-qPCR experiment

Gene name	Primer sequences	
	Forward	Reverse
<i>β-actin</i>	5'-GAGATTACTGCCCT GGCTCCTA-3'	5'-GACTCATCGTACTC CTGCTTGCTG-3'
<i>Bax</i>	5'-AAACTGGTGCTCAAGGCC-3'	5'-GGGTCCCGAAGTAGGAAAGG-3'
<i>Bcl-2</i>	5'-GCTACGAGTGGGATACTGG-3'	5'-GTGTGCAGATGCCGGTTCA-3'
<i>P53</i>	5'-CCAGGGTGGTTGGGTGAGACT-3'	5'-TGGGAGGTCAGCAGGGTAGAT-3'
<i>Caspase-3</i>	5'-GGTATTGAGACAGACAGTGG-3'	5'-CATGGGATCTGTTTCTTTGC-3'
<i>Caspase-9</i>	5'-AGATGCTGTCCCATACCAGG-3'	5'-CAGGAACCGCTCTTCTTGTC-3'

Table 2 Effect of subchronic daily administration of SiNPs at doses of 25 and 100 mg/kg b.w/day for 28 days on hepatic marker levels in rats

Parameters	Groups		
	Control	25 mg SiNPs/kg	100 mg SiNPs/kg
LDH (U/I)	167 ± 15.5	227 ± 22.7*	255 ± 66.7***
ALAT (U/I)	29.4 ± 3.08	38.2 ± 6.44*	45.9 ± 5.32**
ASAT (U/I)	106 ± 39.1	124 ± 15.1*	132 ± 7.14**

^aValues are expressed as mean ± SEM, $n=10$ rats/group. One-way ANOVA-Student followed by Tukey's post hoc test for comparison between SiNP groups with controls; * $p < 0.05$, ** $p < 0.01$, *** $p < 0.001$

(< 25% of sections); (++) , moderate (25–50% of sections); and (+++), severe (51–75% of sections).

Statistical Analysis

Statistical analyses were performed using GraphPad Prism 8.0 for Windows (GraphPad Software, San Diego, CA). Data are presented as mean ± SEM. Significant differences between treatment effects were determined by one-way ANOVA, followed by Tukey's post hoc test for multiple comparisons, while correlation analyses were performed by Pearson correlation test. The level of significance was set at * $p < 0.05$, ** $p < 0.01$, *** $p < 0.001$ between treated groups and controls.

Results

Effect of Silica Nanoparticles on Hepatic Toxicity Serum Markers

Table 2 shows biochemical markers of liver injury in rats after daily subacute exposure to SiNPs at 25 and 100 mg/kg bw. The levels of hepatic enzyme such as alanine aminotransferase (ALAT), aspartate aminotransferase (ASAT), and lactate dehydrogenase (LDH) were significantly ($p < 0.01$) increased in both SiNPs-treated groups compared

to controls. The effect was more accentuated at the higher dose of SiNPs (100 mg/kg bw).

Effect of Silica Nanoparticles on Generation of ROS and NO in the Liver

ROS and NO levels were determined to evaluate the effect of SiNPs on the redox balance in the liver of rats. ROS levels were significantly increased in the liver of rats treated with 25 and 100 mg/kg bw of SiNPs compared to controls ($p < 0.01$ and $p < 0.001$, respectively) (Fig. 1A). NO was also increased in the liver of rats following administration of SiNPs at the dose 100 mg/kg bw compared to controls ($p < 0.001$) (Fig. 1B).

Effect of silica nanoparticles exposure on oxidative stress markers in the liver

Figure 2 shows that SiNP exposure significantly increased MDA, PCO, and H_2O_2 levels in a dose-dependent manner when compared with the control group ($p < 0.001$ for MDA and H_2O_2 between the dose 100 mg/kg bw and controls; $p < 0.01$ for PCO between the dose 100 mg/kg bw and controls as well as for PCO and H_2O_2 between the dose 25 mg/kg bw and controls).

Effect of Silica Nanoparticles on Hepatic Antioxidant Defense System

Results of enzymatic and non-enzymatic antioxidant parameters are presented in Fig. 3. Rats receiving 25 mg/kg bw of SiNPs showed no significant ($p > 0.05$) changes in GSH contents and GPx activity when compared with the control group (Fig. 3A, B). On the other hand, exposure to SiNPs at a dose of 100 mg/kg decreased significantly GSH ($p < 0.05$) and GPx activity ($p < 0.001$) in comparison with the control group. The antioxidant enzyme activities of CAT and SOD were significantly ($p < 0.001$) declined in the liver of SiNP-treated rats at both treatment doses (25 and 100 mg/kg bw) when compared to the control group (Fig. 3C, D).

Fig. 1 Intracellular ROS (A) and NO (B) generation in liver tissues of different experimental rat groups treated i.p. with SiNPs at 25 and 100 mg/kg bw/day for 28 days. Values are expressed as mean \pm SEM, $n = 10$ rats/group. ** = $p < 0.01$ and *** = $p < 0.001$ when comparing SiNP-treated rats with controls

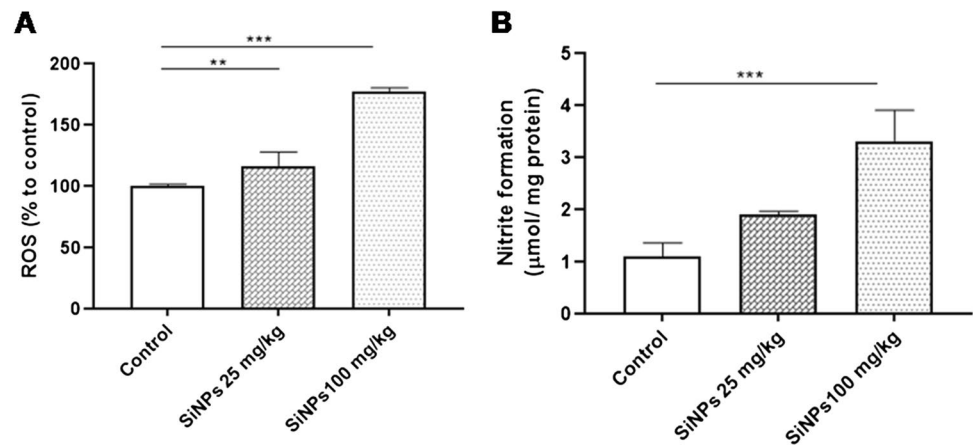
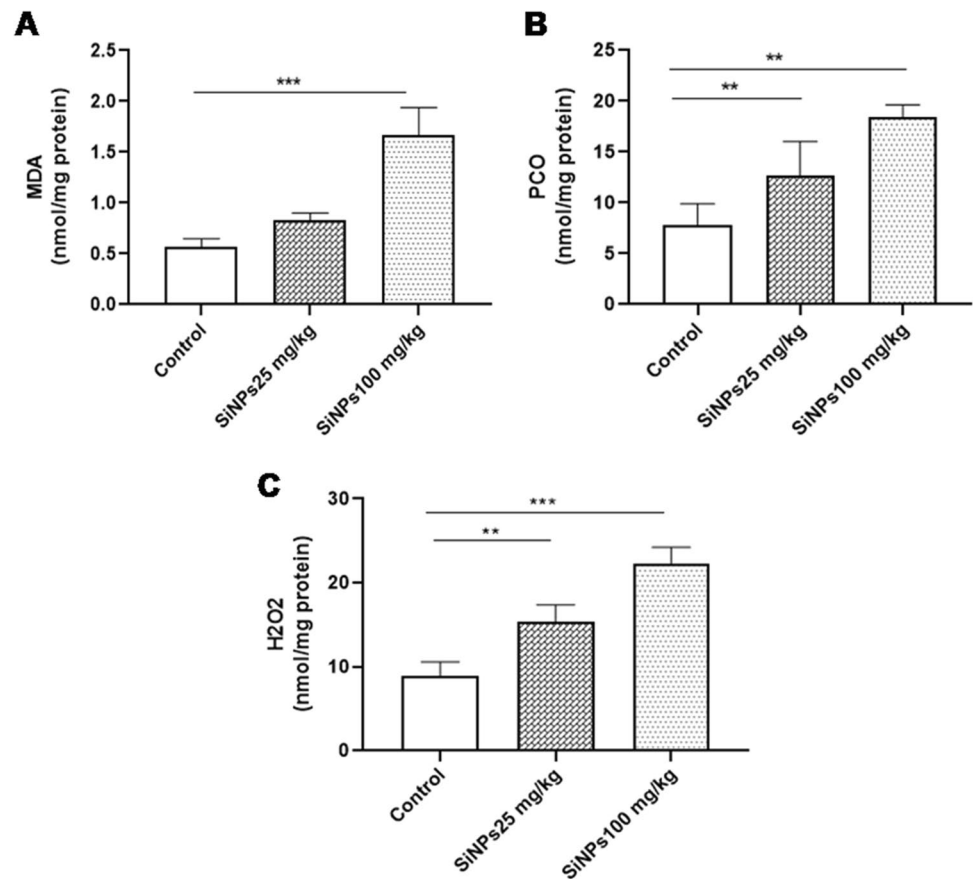


Fig. 2 Effect of i.p. administration of SiNPs at doses of 25 and 100 mg/kg bw/day for 28 days on lipid peroxidation (MDA) (A), protein carbonylation (PCO) (B), and hydroperoxide generation (H_2O_2) (C) in the liver of rats. Values are expressed as mean \pm SEM, $n = 10$ rats/group. ** = $p < 0.01$ and *** = $p < 0.001$ when comparing SiNP-treated rats with controls



Effect of Silica nanoparticles on Apoptosis-Related Gene Expression Levels in Liver

The mRNA level of some apoptotic genes (*p53*, *Bax*, *Bcl-2*, *Casp3*, and *Casp9*) were analyzed in the liver of rats treated with SiNPs (25 and 100 mg/kg bw for 28 days). Results of quantitative real-time PCR (qRT-PCR) showed that SiNP exposure upregulated the expression of pro-apoptotic genes (*p53* and *Bax*) and downregulated the anti-apoptotic gene *Bcl-2* (Fig. 4A, B, and C, respectively). Furthermore, *Bcl-2*/

Bax ratio was significantly decreased in SiNP-treated groups compared to controls (Fig. 4D). The expression of caspase genes (*Casp-3* and *Casp-9*) was significantly increased in the liver of SiNP-treated groups compared to controls (Fig. 4E and F).

The correlational analyses showed that hepatic ROS levels were positively correlated with mRNA levels of *Bax* ($r = 0.957$; $p < 0.001$), *p53* ($r = 0.661$; $p > 0.05$), *caspase-3* ($r = 0.749$; $p < 0.05$), and *caspase-9* ($r = 0.531$; $p < 0.05$) and inversely correlated with the mRNA levels of *Bcl-2* gene

Fig. 3 Effect of i.p. administration of SiNPs at doses of 25 and 100 mg/kg bw/day for 28 days on the enzymatic and non-enzymatic antioxidant activities in the liver of rats: **A** Glutathione (GSH) activity ($\mu\text{mol}/\text{mg}$ protein), **B** glutathione peroxidase (GPx) activity (μmol GSH consumed/min/mg of proteins), **C** catalase (CAT) activity ($\mu\text{mol}/\text{min}/\text{mg}$ of protein), and **D** superoxide dismutase (SOD) activity (U/mg of protein). Values are expressed as mean \pm SEM, $n = 10$ rats/group. * = $p < 0.05$, ** = $p < 0.01$, and *** = $p < 0.001$ when comparing SiNP-treated rats with controls

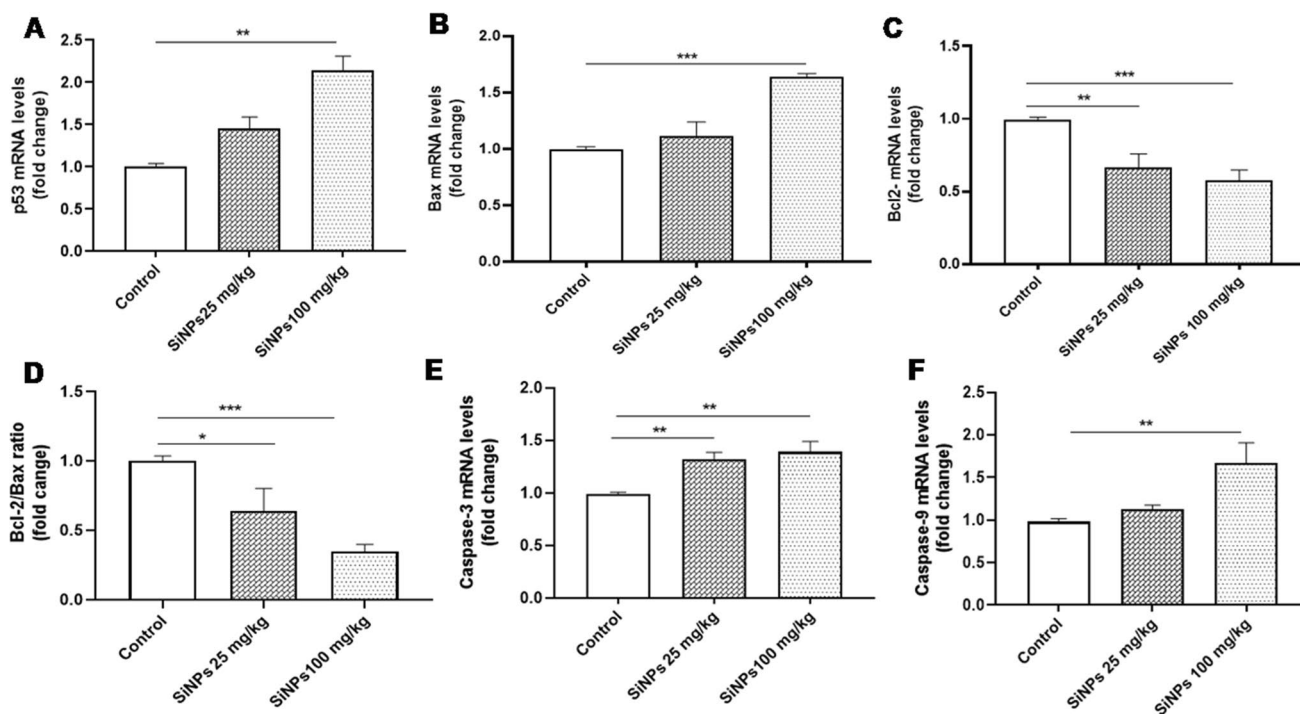
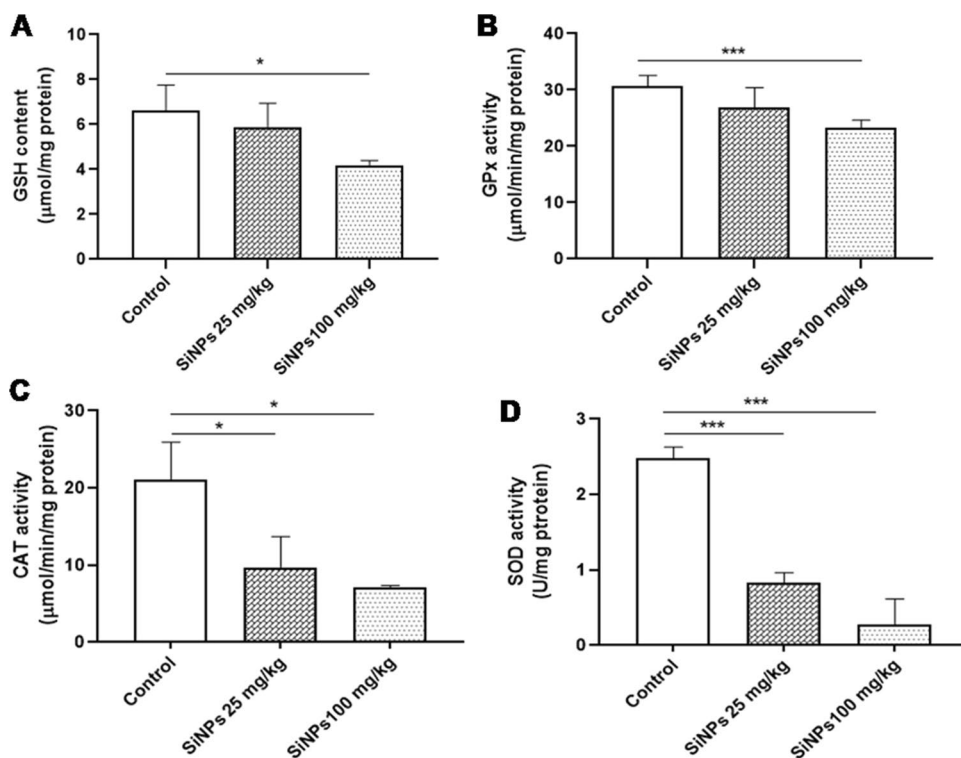


Fig. 4 Effect of i.p. administration of SiNPs at doses of 25 and 100 mg/kg bw/day for 28 days on p53 (A), Bax (B), Bcl-2 (C), Bcl-2/Bax ratio (D), Caspase-3 (E), and Caspase-9 (F) gene expression.

Values are expressed as mean \pm SEM, $n = 6$ rats/group. ** = $p < 0.01$ and *** = $p < 0.001$ when comparing SiNP-treated rats with controls

($r = -0.428$, $p < 0.05$). These results suggest that SiNPs altered the regulation of apoptotic gene expression via ROS generation.

Histological Alterations in the liver Rats after Silica Nanoparticle Exposure

The hepatic effects of SiNPs were confirmed by the histopathological findings (Fig. 5; Table 3). In the control group, no histopathological changes were observed, with regular arrangement along the sinusoids with spherically localized nuclei (Fig. 5a). On the other hand, the group exposed to low-dose SiNPs (25 mg/kg bw) showed abnormal architecture along with dilated sinusoids, Kupffer cell hyperplasia, and infiltration of inflammatory cells (Fig. 5b–d). In the group receiving 100 mg/kg bw SiNPs, there was necrosis (arrow) (e), Kupffer cell hyperplasia (f), sinusoidal dilatation (arrow) (g), and infiltration of inflammatory cells with aggregation of inflammatory cells in the hepatic portal space (arrow) (h).

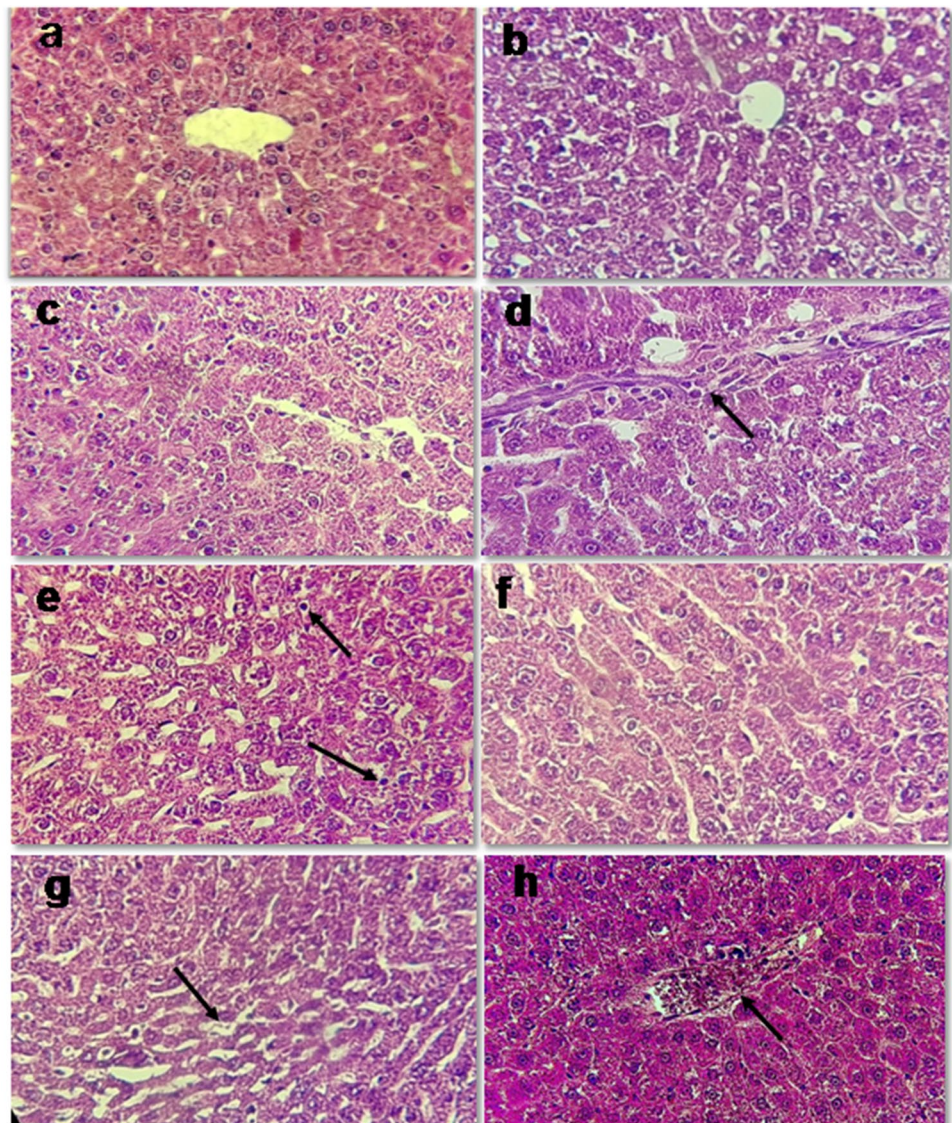
Table 3 Histopathological alterations in rat liver induced by SiNPs after 28 days of daily exposure

	Controls	SiNPs treated rats (mg/kg bw/day)	
		25	100
Kupffer cells hyperplasia	-	++	+++
Sinusoidal dilatation	-	++	+++
Necrotic hepatocytes	-	-	+++
Vacuolar degeneration	-	-	++

(-) No change, (+) mild change, (++) moderate change, and (+++) severe change

(arrow) (g), and infiltration of inflammatory cells with aggregation of inflammatory cells in the hepatic portal space (arrow) (Fig. 5e–h).

Fig. 5 Histopathology of hematoxylin and eosin (H and E, $\times 400$)–stained liver of rats: (a) from the control group showing normal hepatic lobule, central veins, and portal area; b–d receiving 25 mg/kg SiNPs and showing Kupffer cell hyperplasia (b), sinusoidal dilatation and widening of the capillaries lining of the hepatic strands (c), and infiltration of lobular inflammatory cells (mainly lymphocytes) in the lobular hepatic strands (arrow) (d); e–h receiving 100 mg/kg SiNPs and exhibiting necrosis (arrow) (e), Kupffer cell hyperplasia (f), sinusoidal dilatation (arrow) (g), and infiltration of inflammatory cells with aggregation of inflammatory cells in the hepatic portal space (arrow) (h)



Discussion

Inorganic nanoparticles are important environmental pollutants with documented adverse effects on multiple systems, although the specific mechanisms leading to such effects are not fully understood. Inorganic nanoparticles are known to cross epithelial barriers and distribute to the different organs due to their small size [29]. In particular, ingested NPs can cross the small intestine walls and reach the blood, brain, lung, heart, kidney, spleen, liver, intestine, and stomach [59] [13, 47].

In the present study, subacute exposure to SiNPs caused a significant increase in serum ASAT, ALAT, and LDH activities indicating hepatotoxic effects of SiNPs. Elevation of serum aminotransferases activities is important which are markers in the diagnosis of hepatocellular damage and liver diseases [38]. These enzymes normally exist in the hepatocytes, and their presence in blood confirms the deterioration of the cell membrane integrity [46]. In the current work, biochemical results were also correlated with histopathological observation of liver sections, which showed that SiNPs induced sinusoidal dilatation and hyperplasia of Kupffer cells with infiltration of inflammatory cells. According to previous studies, infiltration of inflammatory cells induced by SiNPs (30 mg/kg, 70 nm) may suggest that these particles interact with interstitial hepatic tissues leading to various immune responses [3, 43]. Furthermore, Kupffer cell hyperplasia observed in SiNP-treated groups might be considered a defense mechanism against hepatic oxidative stress [27, 59].

The increase in MDA and PCO levels observed in the current study was further indicative of oxidative damage in the tissue caused by the SiNPs, leading to the release of lipid peroxidation and protein oxidation products, which can impair cell function [41, 50]. This generation of ROS and oxidative stress response is in fact an important mechanism observed in response to exposure to a variety of nanomaterials [1, 57]. These data are in agreement with previous studies that confirmed the involvement of oxidative stress and lipid peroxidation in SiNPs-induced hepatic and renal toxicity [36, 58].

Accordingly, the observed increase in nitric oxide (NO) levels in the liver could be attributed to the activation of NO synthase enzyme by SiNPs. The most important feature of NO is its ability to react with superoxide anion

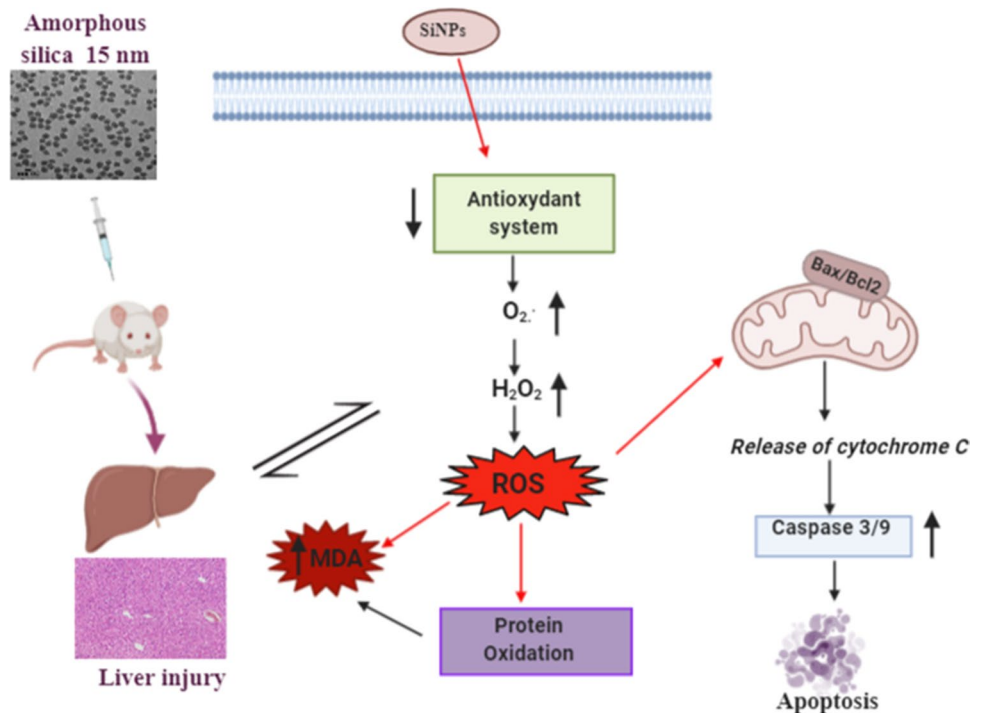
(O₂⁻) to generate peroxynitrite (ONOO⁻), a potent oxidant that causes oxidative DNA damage and cell injury by oxidizing and nitrating cellular macromolecules [30, 35].

Furthermore, the decrease in GSH levels observed in SiNP-treated groups may have occurred as a result of its consumption in scavenging the increased ROS and NO species. Under normal conditions, the overproduction of ROS is neutralized by the antioxidant defense mechanisms, which induces both enzymatic and non-enzymatic antioxidants. Reduced glutathione, a major endogenous antioxidant, plays an important role in protecting cells against oxidative stress by direct scavenging of free radicals or serving as a substrate for some antioxidant enzymes (like thioredoxin, glutathione peroxidase, and glutathione-S-transferases) by accepting or donating hydrogen atoms [9]. Moreover, our study showed a decline in antioxidant enzyme activities (CAT, SOD, GPx) in SiNP-treated rats. These findings confirmed that SiNP-induced oxidative stress is not only attributed to excessive production of toxic oxygen metabolites but also results from the deterioration of antioxidant defense mechanisms.

Finally, our findings clearly revealed that exposure to SiNPs triggers apoptosis in liver tissues by activating the Bax/Bcl2 and caspase-3 pathway. Hepatocyte apoptosis has been documented as a major mechanism caused by NP-induced oxidative stress [19]. It is well known that apoptosis is a regulated form of cellular death, with several checkpoints and mediators, activated through extrinsic and intrinsic pathways [55]. Apoptosis signaling pathways involve Bax as a proapoptotic protein and Bcl-2 as an anti-apoptotic protein. Mitochondria rapidly collapse their membrane potential ($\Delta\Psi_m$) and generate ROS, contributing to the release of cytochrome c, which activates the caspase signaling to initiate cell death. In this study, we demonstrated that SiNPs downregulated Bcl-2 expression and upregulated Bax, p53, and both the caspase-3/9 expressions (apoptotic initiator and executioners). These results are in accordance with previous studies, which revealed that nanoparticles activate apoptotic signaling [52].

In conclusion, the results of the present study suggest that subacute exposure of male rats to SiNP-induced hepatotoxicity as evidenced by an increase in oxidative stress markers, as well as induction of apoptotic (Bax/Bcl2/Casp3/9) gene expressions, associated with histological alterations (Fig. 6).

Fig. 6 Proposed schematic diagram illustrating SiNP-induced hepatic toxicity and apoptosis



Author Contribution BA, KB, BG, and HF participated in the research design. The experiments were performed by BA, and KB. Data were analyzed by BA, KB, BG, and HF. AA contributed to histology analysis. BA, BG, and HF contributed to the writing of the manuscript. In addition, BA, KB, BG, HSB, MK, MB, and HF reviewed the data and the manuscript. All authors have read and approved the final version of the manuscript.

Funding This work was financially supported by the “PRD program for Research and innovation between the Tunisian Ministry of higher education and scientific research and the Kingdom of Morocco Ministry of National Education and Vocational Training “ PRD project number 20/PRD-10.”

Availability of Data and Materials Not applicable.

Declarations

Ethics Approval and Consent to Participate The experimental approach and handling of animals were performed under the experiments conducted approved by the Ethical Committee Guidelines for the Care and Use of Laboratory Animals of the Faculty of Sciences of Sfax, Tunisia. It was also carried out following guidelines as set out in the “Guide for the Care and Use of Laboratory Animals” and with the authorization of the committee.

Consent for Publication Not applicable.

Conflict of Interest The authors declare no competing interests.

References

- Abdelazeim SA, Shehata NI, Aly HF, Shams SGE (2020) Amelioration of oxidative stress-mediated apoptosis in copper oxide nanoparticles-induced liver injury in rats by potent antioxidants. *Sci Rep* 10:10812. <https://doi.org/10.1038/s41598-020-67784-y>
- Aebi, H., 1984. [13] Catalase in vitro, in: *Methods in Enzymology*. Elsevier, pp. 121–126. [https://doi.org/10.1016/S0076-6879\(84\)05016-3](https://doi.org/10.1016/S0076-6879(84)05016-3)
- Ahmed MA (2013) The protective effect of ginger (*Zingiber officinale*) against adriamycin-induced hepatotoxicity in rats: histological study. *Life Sci J* 10(1):1412–1422
- Alkan, F.Ü., Gürsel, F.E., Ateş, A., Özyürek, M., Güçlü, K., Altun, M., 2012. Protective effects of *Salvia officinalis* extract against cyclophosphamide-induced genotoxicity and oxidative stress in rats 9.
- Almansour M, Alarifi S, Jarrar B (2018) In vivo investigation on the chronic hepatotoxicity induced by intraperitoneal administration of 10-nm silicon dioxide nanoparticles. *IJN* 13:2685–2696. <https://doi.org/10.2147/IJN.S162847>
- Aouey, B., Fares, E., Chtourou, Y., Bouchard, M., Fetoui, H., 2019. Lambda-cyhalothrin exposure alters purine nucleotide hydrolysis and nucleotidase gene expression pattern in platelets and liver of rats. *Chem Biol Interact* 311 108796. <https://doi.org/10.1016/j.cbi.2019.108796>
- Attardi LD, Reczek EE, Cosmas C, Demicco EG, McCurrach ME, Lowe SW, Jacks T (2000) PERP, an apoptosis-associated target of p53, is a novel member of the PMP-22/gas3 family. *Genes Dev* 14:704–718
- Balli, E., Yalin, S., Eroğlu, P., Bayrak, G., Çömelekoğlu, Ü., 2019. Effects of different sizes silica nanoparticle on the liver, kidney and brain in rats: biochemical and histopathological evaluation. *jrp* 23, 344–353. <https://doi.org/10.12991/jrp.2019.142>

9. Birk J, Meyer M, Aller I, Hansen HG, Odermatt A, Dick TP, Meyer AJ, Appenzeller-Herzog C (2013) Endoplasmic reticulum: reduced and oxidized glutathione revisited. *J Cell Sci* 126:1604–1617. <https://doi.org/10.1242/jcs.117218>
10. Bradford MM (1976) A rapid and sensitive method for the quantitation of microgram quantities of protein utilizing the principle of protein-dye binding. *Anal Biochem* 72:248–254. [https://doi.org/10.1016/0003-2697\(76\)90527-3](https://doi.org/10.1016/0003-2697(76)90527-3)
11. Chan W-T, Liu C-C, Chiang Chiau J-S, Tsai S-T, Liang C-K, Cheng M-L, Lee H-C, Yeung C-Y, Hou S-Y (2017) In vivo toxicologic study of larger silica nanoparticles in mice. *IJN* 12:3421–3432. <https://doi.org/10.2147/IJN.S126823>
12. Dilberoglu UM, Gharehpapagh B, Yaman U, Dolen M (2017) The role of additive manufacturing in the era of Industry 4.0. *Procedia Manufacturing* 11:545–554. <https://doi.org/10.1016/j.promfg.2017.07.148>
13. Dogra P, Adolphi NL, Wang Z, Lin Y-S, Butler KS, Durfee PN, Croissant JG, Noureddine A, Coker EN, Bearer EL, Cristini V, Brinker CJ (2018) Establishing the effects of mesoporous silica nanoparticle properties on in vivo disposition using imaging-based pharmacokinetics. *Nat Commun* 9:4551. <https://doi.org/10.1038/s41467-018-06730-z>
14. Draper, H.H., Hadley, M., 1990. [43] Malondialdehyde determination as index of lipid peroxidation, in: *Methods in Enzymology*. Elsevier, pp. 421–431. [https://doi.org/10.1016/0076-6879\(90\)86135-1](https://doi.org/10.1016/0076-6879(90)86135-1)
15. Driver AS, Kodavanti PRS, Mundy WR (2000) Age-related changes in reactive oxygen species production in rat brain homogenates. *Neurotoxicol Teratol* 22:175–181. [https://doi.org/10.1016/S0892-0362\(99\)00069-0](https://doi.org/10.1016/S0892-0362(99)00069-0)
16. Du Z, Chen S, Cui G, Yang Y, Zhang E, Wang Q, Lavin M, Yeo A, Bo C, Zhang Y, Li C, Liu X, Yang X, Peng C, Shao H (2018) Silica nanoparticles induce cardiomyocyte apoptosis via the mitochondrial pathway in rats following intratracheal instillation. *Int J Mol Med*. <https://doi.org/10.3892/ijmm.2018.4045>
17. Ellman GL (1959) Tissue sulfhydryl groups. *Arch Biochem Biophys* 82:70–77. [https://doi.org/10.1016/0003-9861\(59\)90090-6](https://doi.org/10.1016/0003-9861(59)90090-6)
18. Elmore S (2007) Apoptosis: a review of programmed cell death. *Toxicol Pathol* 35:495–516. <https://doi.org/10.1080/01926230701320337>
19. Eom H-J, Choi J (2010) p38 MAPK activation, DNA damage, cell cycle arrest and apoptosis as mechanisms of toxicity of silver nanoparticles in Jurkat T cells. *Environ Sci Technol* 44:8337–8342. <https://doi.org/10.1021/es1020668>
20. Farnebo M, Bykov VJN, Wiman KG (2010) The p53 tumor suppressor: a master regulator of diverse cellular processes and therapeutic target in cancer. *Biochem Biophys Res Commun* 396:85–89. <https://doi.org/10.1016/j.bbrc.2010.02.152>
21. Fetoui H, Mahjoubi-Samet A, Jammousi K, Ellouze F, Guermazi F, Zeghal N (2006) Energy restriction in pregnant and lactating rats lowers bone mass of their progeny. *Nutr Res* 26:421–426. <https://doi.org/10.1016/j.nutres.2006.06.016>
22. Flohé, L., Günzler, W.A., 1984. [12] Assays of glutathione peroxidase, in: *Methods in Enzymology*. Elsevier, pp. 114–120. [https://doi.org/10.1016/S0076-6879\(84\)05015-1](https://doi.org/10.1016/S0076-6879(84)05015-1)
23. Gay C, Collins J, Gebicki JM (1999) Determination of iron in solutions with the ferric-xylene orange complex. *Anal Biochem* 273:143–148. <https://doi.org/10.1006/abio.1999.4207>
24. Green LC, Wagner DA, Glogowski J, Skipper PL, Wishnok JS, Tannenbaum SR (1982) Analysis of nitrate, nitrite, and [15N] nitrate in biological fluids. *Anal Biochem* 126:131–138. [https://doi.org/10.1016/0003-2697\(82\)90118-X](https://doi.org/10.1016/0003-2697(82)90118-X)
25. Guo C, Xia Y, Niu P, Jiang L, Duan J, Yu Y, Zhou X, Li Y, Sun Z (2015) Silica nanoparticles induce oxidative stress, inflammation, and endothelial dysfunction in vitro via activation of the MAPK/Nrf2 pathway and nuclear factor- κ B signaling. *IJN* 1463. <https://doi.org/10.2147/IJN.S76114>
26. Gupta S, Kass GEN, Szegezdi E, Joseph B (2009) The mitochondrial death pathway: a promising therapeutic target in diseases. *J Cell Mol Med* 13:1004–1033. <https://doi.org/10.1111/j.1582-4934.2009.00697.x>
27. Ivanov S, Zhuravsky S, Yukina G, Tomson V, Korolev D, Galagudza M (2012) In vivo toxicity of intravenously administered silica and silicon nanoparticles. *Materials* 5:1873–1889. <https://doi.org/10.3390/ma5101873>
28. Kanipandian N, Li D, Kannan S (2019) Induction of intrinsic apoptotic signaling pathway in A549 lung cancer cells using silver nanoparticles from *Gossypium hirsutum* and evaluation of in vivo toxicity. *Biotechnol Rep* 23:e00339. <https://doi.org/10.1016/j.btre.2019.e00339>
29. Kim J-H, Kim C-S, Ignacio RM, Kim D-H, Sajo MEJ, Maeng E, Qi X-F, Park S-E, Kim Y-R, Kim M-K, Lee K-J, Kim S-K (2014) Immunotoxicity of silicon dioxide nanoparticles with different sizes and electrostatic charge. *Int J Nanomed* 9(Suppl 2):183–193. <https://doi.org/10.2147/IJN.S57934>
30. Korhonen R, Lahti A, Kankaanranta H, Moilanen E (2005) Nitric oxide production and signaling in inflammation. *Curr Drug Targets Inflamm Allergy* 4:471–479. <https://doi.org/10.2174/1568010054526359>
31. Kumar, S., Eroglu, E., Stokes, J.A., Scissum-Gunn, K., Saldanha, S.N., Singh, U.P., Manne, U., Ponnazhagan, S., Mishra, M.K., 2017. Resveratrol induces mitochondria-mediated, caspase-independent apoptosis in murine prostate cancer cells. *Oncotarget* 8, 20895–20908. <https://doi.org/10.18632/oncotarget.14947>
32. Li J, He X, Yang Y, Li M, Xu C, Yu R (2018) Risk assessment of silica nanoparticles on liver injury in metabolic syndrome mice induced by fructose. *Sci Total Environ* 628–629:366–374. <https://doi.org/10.1016/j.scitotenv.2018.02.047>
33. LJVAK, K., (2001) Analysis of relative gene expression data using real time quantitative PCR and the $2^{-\Delta\Delta CT}$ method. *Methods* 25:402–408
34. Ly, J.D., Grubb, D.R., Lawen, A., 2003. The mitochondrial membrane potential ($\Delta\psi_m$) in apoptosis; an update 14.
35. Mahmoud AM, Dera HSA (2015) 18 β -Glycyrrhetic acid exerts protective effects against cyclophosphamide-induced hepatotoxicity: potential role of PPAR γ and Nrf2 upregulation. *Genes Nutr* 10:1–13. <https://doi.org/10.1007/s12263-015-0491-1>
36. Mahmoud AM, Desouky EM, Hozayen WG, Bin-Jumah M, El-Nahass E-S, Soliman HA, Farghali AA (2019) Mesoporous silica nanoparticles trigger liver and kidney injury and fibrosis via altering TLR4/NF- κ B, JAK2/STAT3 and Nrf2/HO-1 signaling in rats. *Biomolecules* 9:528. <https://doi.org/10.3390/biom9100528>
37. Marklund S, Marklund G (1974) Involvement of the superoxide anion radical in the autoxidation of pyrogallol and a convenient assay for superoxide dismutase. *Eur J Biochem* 47:469–474. <https://doi.org/10.1111/j.1432-1033.1974.tb03714.x>
38. McGill, M.R., 2016. The past and present of serum aminotransferases and the future of liver injury biomarkers. *EXCLI J* 15, 817–828. <https://doi.org/10.17179/excli2016-800>
39. Michael T (2008) Progress in the development of microscopical techniques for diagnostic pathology. *J Histotechnol* 32:9–19. <https://doi.org/10.1179/his.2009.32.1.9>
40. Murugadoss S, Lison D, Godderis L, Van Den Brule S, Mast J, Brassinne F, Sebaihi N, Hoet PH (2017) Toxicology of silica nanoparticles: an update. *Arch Toxicol* 91:2967–3010. <https://doi.org/10.1007/s00204-017-1993-y>
41. Napierska D, Thomassen LC, Lison D, Martens JA, Hoet PH (2010) The nanosilica hazard: another variable entity. *Part Fibre Toxicol* 7:39. <https://doi.org/10.1186/1743-8977-7-39>
42. Nemmar A, Yuvaraju P, Beegam S, Pathan J, Kazzam EE, Ali BH (2016) Oxidative stress, inflammation, and DNA damage

- in multiple organs of mice acutely exposed to amorphous silica nanoparticles. *IJN* 919. <https://doi.org/10.2147/IJN.S92278>
43. Nishimori H, Kondoh M, Isoda K, Tsunoda S, Tsutsumi Y, Yagi K (2009) Silica nanoparticles as hepatotoxicants. *Eur J Pharm Biopharm* 72:496–501. <https://doi.org/10.1016/j.ejpb.2009.02.005>
 44. Parrish AB, Freel CD, Kornbluth S (2013) Cellular mechanisms controlling caspase activation and function. *Cold Spring Harb Perspect Biol* 5:a008672–a008672. <https://doi.org/10.1101/cshperspect.a008672>
 45. Pathak G, Singh S, Kumari P, Hussain Y, Raza W, Luqman S, Meena A (2020) Cirsilineol inhibits proliferation of lung squamous cell carcinoma by inducing ROS mediated apoptosis. *Food Chem Toxicol* 143:111550. <https://doi.org/10.1016/j.fct.2020.111550>
 46. Ramaiah SK (2007) A toxicologist guide to the diagnostic interpretation of hepatic biochemical parameters. *Food Chem Toxicol* 45:1551–1557. <https://doi.org/10.1016/j.fct.2007.06.007>
 47. Rambanapasi C, Zeevaart J, Bunting H, Bester C, Kotze D, Hayeshi R, Grobler A (2016) Bioaccumulation and subchronic toxicity of 14 nm gold nanoparticles in rats. *Molecules* 21:763. <https://doi.org/10.3390/molecules21060763>
 48. Reznick, A.Z., Packer, L., 1994. [38] Oxidative damage to proteins: spectrophotometric method for carbonyl assay, in: *Methods in Enzymology, Oxygen Radicals in Biological Systems Part C*. Academic Press, pp. 357–363. [https://doi.org/10.1016/S0076-6879\(94\)33041-7](https://doi.org/10.1016/S0076-6879(94)33041-7)
 49. Roshanfekrnahzomi Z, Badpa P, Esfandiari B, Taheri S, Nouri M, Akhtari K, Shahpasand K, Falahati M (2019) Silica nanoparticles induce conformational changes of tau protein and oxidative stress and apoptosis in neuroblastoma cell line. *Int J Biol Macromol* 124:1312–1320. <https://doi.org/10.1016/j.ijbiomac.2018.09.118>
 50. Sureshbabu A, Ryter SW, Choi ME (2015) Oxidative stress and autophagy: crucial modulators of kidney injury. *Redox Biol* 4:208–214. <https://doi.org/10.1016/j.redox.2015.01.001>
 51. Van der Zande, M.; Vandebriel, R.J.; Groot, M.J.; Kramer, E.; Herrera Rivera, Z.E.; Rasmussen, K.; Ossenkoppele, J.S.; Tromp, P.; Gremmer, E.R.; Peters, R.J.B.; et al. Sub-chronic toxicity study in rats orally exposed to nanostructured silica. *Part. Fibre Toxicol.* 2014, 11, 8. <https://doi.org/10.1186/1743-8977-11-8>.
 52. Wang H, Zhang F, Wen H, Shi W, Huang Q, Huang Y, Xie J, Li P, Chen J, Qin L, Zhou Y (2020) Tumor- and mitochondria-targeted nanoparticles eradicate drug resistant lung cancer through mitochondrial pathway of apoptosis. *J Nanobiotechnol* 18:8. <https://doi.org/10.1186/s12951-019-0562-3>
 53. Wang L, Hu C, Shao L (2017) The antimicrobial activity of nanoparticles: present situation and prospects for the future. *IJN* 12:1227–1249. <https://doi.org/10.2147/IJN.S121956>
 54. Williams A.B, Schumacher B (2016) p53 in the DNA-damage-repair process. *Cold Spring Harb Perspect Med* 6:a026070. <https://doi.org/10.1101/cshperspect.a026070>
 55. Xia T, Kovoichich M, Brant J, Hotze M, Sempf J, Oberley T, Sioutas C, Yeh JI, Wiesner MR, Nel AE (2006) Comparison of the abilities of ambient and manufactured nanoparticles to induce cellular toxicity according to an oxidative stress paradigm. *Nano Lett* 6:1794–1807. <https://doi.org/10.1021/nl061025k>
 56. Yang L, Kuang H, Zhang W, Aguilar ZP, Wei H, Xu H (2017) Comparisons of the biodistribution and toxicological examinations after repeated intravenous administration of silver and gold nanoparticles in mice. *Sci Rep* 7:3303. <https://doi.org/10.1038/s41598-017-03015-1>
 57. Yousef MI, Mutar TF, Kamel MAE-N (2019) Hepato-renal toxicity of oral sub-chronic exposure to aluminum oxide and/or zinc oxide nanoparticles in rats. *Toxicol Rep* 6:336–346. <https://doi.org/10.1016/j.toxrep.2019.04.003>
 58. Yu Y, Duan J, Li Y, Li Y, Jing L, Yang M, Wang J, Sun Z (2017) Silica nanoparticles induce liver fibrosis via TGF- β ₁/Smad3 pathway in ICR mice. *IJN* 12:6045–6057. <https://doi.org/10.2147/IJN.S132304>
 59. Yu Yang, Li Yang, Wang W, Jin M, Du Z, Li Yanbo, Duan J, Yu Yongbo, Sun Z (2013) Acute toxicity of amorphous silica nanoparticles in intravenously exposed ICR mice. *PLoS ONE* 8:e61346. <https://doi.org/10.1371/journal.pone.0061346>
 60. Zhang X, Luan J, Chen W, Fan J, Nan Y, Wang Y, Liang Y, Meng G, Ju D (2018) Mesoporous silica nanoparticles induced hepatotoxicity via NLRP3 inflammasome activation and caspase-1-dependent pyroptosis. *Nanoscale* 10:9141–9152. <https://doi.org/10.1039/C8NR00554K>
 61. Zhang Y, Bai Y, Jia J, Gao N, Li Y, Zhang R, Jiang G, Yan B (2014) Perturbation of physiological systems by nanoparticles. *Chem Soc Rev* 43:3762–3809. <https://doi.org/10.1039/C3CS60338E>

Publisher's Note Springer Nature remains neutral with regard to jurisdictional claims in published maps and institutional affiliations.